Hindawi Publishing Corporation
EURASIP Journal on Wireless Communications and Networking
Volume 2007, Article ID 45084, 10 pages
doi:10.1155/2007/45084

Research Article

Optimal Design of Uniform Rectangular Antenna Arrays for Strong Line-of-Sight MIMO Channels

Frode Bøhagen,[1] Pål Orten,[2] and Geir Øien[3]

[1] *Telenor Research and Innovation, Snarøyveien 30, 1331 Fornebu, Norway*
[2] *Department of Informatics, UniK, University of Oslo (UiO) and Thrane & Thrane, 0316 Oslo, Norway*
[3] *Department of Electronics and Telecommunications, Norwegian University of Science and Technology (NTNU), 7491 Trandheim, Norway*

Received 26 October 2006; Accepted 1 August 2007

Recommended by Robert W. Heath

We investigate the optimal design of *uniform rectangular arrays* (URAs) employed in *multiple-input multiple-output* communications, where a strong *line-of-sight* (LOS) component is present. A general geometrical model is introduced to model the LOS component, which allows for any orientation of the transmit and receive arrays, and incorporates the uniform linear array as a special case of the URA. A spherical wave propagation model is used. Based on this model, we derive the optimal array design equations with respect to mutual information, resulting in orthogonal LOS subchannels. The equations reveal that it is the distance between the antennas projected onto the plane perpendicular to the transmission direction that is of importance with respect to design. Further, we investigate the influence of nonoptimal design, and derive analytical expressions for the singular values of the LOS matrix as a function of the quality of the array design. To evaluate a more realistic channel, the LOS channel matrix is employed in a Ricean channel model. Performance results show that even with some deviation from the optimal design, we get better performance than in the case of uncorrelated Rayleigh subchannels.

1. INTRODUCTION

Multiple-input multiple-output (MIMO) technology is a promising tool for enabling spectrally efficient future wireless applications. A lot of research effort has been put into the MIMO field since the pioneering work of Foschini and Gans [1] and Telatar [2], and the technology is already hitting the market [3, 4]. Most of the work on wireless MIMO systems seek to utilize the decorrelation between the subchannels introduced by the multipath propagation in the wireless environment [5]. Introducing a strong *line-of-sight* (LOS) component for such systems is positive in the sense that it boosts the *signal-to-noise ratio* (SNR). However, it will also have a negative impact on MIMO performance as it increases the correlation between the subchannels [6].

In [7], the possibility of enhancing performance by proper antenna array design for MIMO channels with a strong LOS component was investigated, and it was shown that the performance can actually be made superior for pure LOS subchannels compared to fully decorrelated Rayleigh subchannels with equal SNR. The authors of the present paper have previously studied the optimal design of *uniform linear arrays* (ULAs) with respect to *mutual information* (MI) [8, 9], and have given a simple equation for the optimal design. Furthermore, some work on the design of *uniform rectangular arrays* (URAs) for MIMO systems is presented in [10], where the optimal design for the special case of two broadside URAs is found, and the optimal throughput performance was identified to be identical to the optimal Hadamard bound. The design is based on taking the spherical nature of the electromagnetic wave propagation into account, which makes it possible to achieve a high rank LOS channel matrix [11]. Examples of real world measurements that support this theoretical work can be found in [12, 13].

In this paper, we extend our work from [8], and use the same general procedure to investigate URA design. We introduce a new general geometrical model that can describe any orientation of the transmit (Tx), receive (Rx) URAs, and also incorporate ULAs as a special case. Again, it should be noted that a spherical wave propagation model is employed, in contrast to the more commonly applied approximate plane-wave model. This model is used to derive new equations for the

optimal design of the URAs with respect to MI. The results are more general than those presented in an earlier work, and the cases of two ULAs [8] and two broadside URAs [10] can be identified as two special cases. The proposed principle is best suited for fixed systems, for example, fixed wireless access and radio relay systems, because the optimal design is dependent on the Tx-Rx distance and on the orientation of the two URAs. Furthermore, we include an analysis of the influence of nonoptimal design, and analytical expressions for the singular values of the LOS matrix are derived as a function of the quality of the array design. The results are useful for system designers both when designing new systems, as well as when evaluating the performance of existing systems.

The rest of the paper is organized as follows. Section 2 describes the system model used. In Section 3, we present the geometrical model from which the general results are derived. The derivation of the optimal design equations is given in Section 4, while the eigenvalues of the LOS channel matrix are discussed in Section 5. Performance results are shown in Section 6, while conclusions are drawn in Section 7.

2. SYSTEM MODEL

The wireless MIMO transmission system employs N Tx antennas and M Rx antennas when transmitting information over the channel. Assuming *slowly varying* and *frequency-flat* fading channels, we model the MIMO transmission in complex baseband as [5]

$$\mathbf{r} = \sqrt{\eta} \cdot \mathbf{H}\mathbf{s} + \mathbf{n}, \tag{1}$$

where $\mathbf{r} \in \mathbb{C}^{M\times 1}$ is the received signal vector, $\mathbf{s} \in \mathbb{C}^{N\times 1}$ is the transmitted signal vector, $\mathbf{H} \in \mathbb{C}^{M\times N}$ is the normalized channel matrix linking the Tx antennas with the Rx antennas, η is the common power attenuation over the channel, and $\mathbf{n} \in \mathbb{C}^{M\times 1}$ is the additive white Gaussian noise (AWGN) vector. $\mathbf{n}$ contains i.i.d. circularly symmetric complex Gaussian elements with zero mean and variance σ_n^2, that is, $\mathbf{n} \sim \mathcal{CN}(\mathbf{0}_{M\times 1}, \sigma_n^2 \cdot \mathbf{I}_M)$,[1] where $\mathbf{I}_M$ is the $M \times M$ identity matrix.

As mentioned above, $\mathbf{H}$ is the normalized channel matrix, which implies that each element in $\mathbf{H}$ has unit average power; consequently, the average SNR is independent of $\mathbf{H}$. Furthermore, it is assumed that the total transmit power is P, and all the subchannels experience the same path loss as accounted for in η, resulting in the total average received SNR at one Rx antenna being $\overline{\gamma} = \eta P/\sigma_n^2$. We apply $\mathbf{s} \sim \mathcal{CN}(\mathbf{0}_{N\times 1}, (P/N) \cdot \mathbf{I}_N)$, which means that the MI of a MIMO transmission described by (1) becomes [2][2]

$$\mathcal{I} = \sum_{p=1}^{U} \log_2\left(1 + \frac{\overline{\gamma}}{N}\mu_p\right) \quad \text{bps/Hz}, \tag{2}$$

where $U = \min(M, N)$ and μ_p is the pth eigenvalue of $\mathbf{W}$ defined as

$$\mathbf{W} = \begin{cases} \mathbf{H}\mathbf{H}^H, & M \le N, \\ \mathbf{H}^H\mathbf{H}, & M > N, \end{cases} \tag{3}$$

where $(\cdot)^H$ is the Hermitian transpose operator.[3]

One way to model the channel matrix is as a sum of two components: a LOS component: and an *non-LOS* (NLOS) component. The ratio between the power of the two components gives the Ricean K-factor [15, page 52]. We express the normalized channel matrix in terms of K as

$$\mathbf{H} = \sqrt{\frac{K}{1+K}} \cdot \mathbf{H}_{\text{LOS}} + \sqrt{\frac{1}{1+K}} \cdot \mathbf{H}_{\text{NLOS}}, \tag{4}$$

where $\mathbf{H}_{\text{LOS}}$ and $\mathbf{H}_{\text{NLOS}}$ are the channel matrices containing the LOS and NLOS channel responses, respectively. In this paper, $\mathbf{H}_{\text{NLOS}}$ is modeled as an *uncorrelated* Rayleigh matrix, that is, $\text{vec}(\mathbf{H}_{\text{NLOS}}) \sim \mathcal{CN}(\mathbf{0}_{MN\times 1}, \mathbf{I}_{MN})$, where $\text{vec}(\cdot)$ is the matrix vectorization (stacking the columns on top of each other). In the next section, the entries of $\mathbf{H}_{\text{LOS}}$ will be described in detail, while in the consecutive sections, the connection between the URA design and the properties of $\mathbf{H}_{\text{LOS}}$ will be addressed. The influence of the stochastic channel component $\mathbf{H}_{\text{NLOS}}$ on performance is investigated in the results section.

3. THE LOS CHANNEL: GEOMETRICAL MODEL

When investigating $\mathbf{H}_{\text{LOS}}$ in this section, we only consider the direct components between the Tx and Rx. The optimal design, to be presented in Section 4, is based on the fact that the LOS components from each of the Tx antennas arrive at the Rx array with a spherical wavefront. Consequently, the common approximate plane wave model, where the Tx and Rx arrays are assumed to be points in space, is not applicable [11]; thus an important part of the contribution of this paper is to characterize the received LOS components.

The principle used to model $\mathbf{H}_{\text{LOS}}$ is *ray-tracing* [7]. Ray-tracing is based on finding the path lengths from each of the Tx antennas to each of the Rx antennas, and employing these path lengths to find the corresponding received phases. We will see later how these path lengths characterize $\mathbf{H}_{\text{LOS}}$, and thus its rank and the MI.

To make the derivation in Section 4 more general, we do not distinguish between the Tx and the Rx, but rather the side with the most antennas and the side with the fewest antennas (the detailed motivation behind this decision is given in the first paragraph of Section 4). We introduce the notation $V = \max(M, N)$, consequently we refer to the side with V antennas as the Vx, and the side with U antennas as the Ux.

We restrict the antenna elements, both at the Ux and at the Vx, to be placed in plane URAs. Thus the antennas are

[1] $\mathcal{CN}(\mathbf{x}, \mathbf{Y})$ denotes a complex symmetric Gaussian distributed random vector, with mean vector $\mathbf{x}$ and covariance matrix $\mathbf{Y}$.

[2] Applying equal power Gaussian distributed inputs in the MIMO system is capacity achieving in the case of a Rayleigh channel, but not necessarily in the Ricean channel case studied here [14]; consequently, we use the term MI instead of capacity.

[3] μ_p also corresponds to the pth singular value of $\mathbf{H}$ squared.

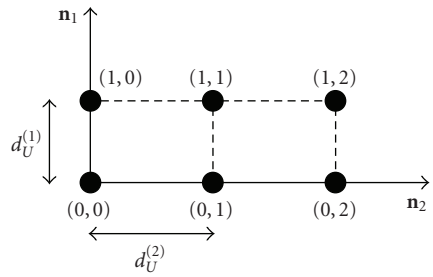

Figure 1: An example of a Ux URA with $U = 6$ antennas ($U_1 = 2$ and $U_2 = 3$).

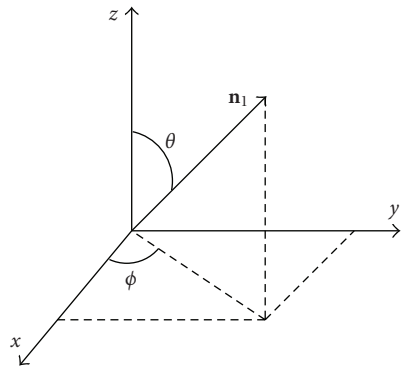

Figure 2: Geometrical illustration of the first principal direction of the URA.

placed on lines going in two orthogonal *principal directions*, forming a lattice structure. The two principal directions are characterized with the vectors $\mathbf{n}_1$ and $\mathbf{n}_2$, while the uniform separation in each direction is denoted by $d^{(1)}$ and $d^{(2)}$. The numbers of antennas at the Ux in the first and second principal directions are denoted by U_1 and U_2, respectively, and we have $U = U_1 \cdot U_2$. The position of an antenna in the lattice is characterized by its index in the first and second principal direction, that is, (u_1, u_2), where $u_1 \in \{0, \ldots, U_1 - 1\}$ and $u_2 \in \{0, \ldots, U_2 - 1\}$. As an example, we have illustrated a Ux array with $U_1 = 2$ and $U_2 = 3$ in Figure 1. The same definitions are used at the Vx side for V_1, V_2, v_1, and v_2.

The path length between Ux antenna (u_1, u_2) and Vx antenna (v_1, v_2) is denoted by $l_{(v_1,v_2)(u_1,u_2)}$ (see Figure 4). Since the elements of $\mathbf{H}_{\text{LOS}}$ are assumed normalized as mentioned earlier, the only parameters of interest are the received phases. The elements of $\mathbf{H}_{\text{LOS}}$ then become

$$(\mathbf{H}_{\text{LOS}})_{m,n} = e^{(j2\pi/\lambda) l_{(v_1,v_2)(u_1,u_2)}}, \tag{5}$$

where $(\cdot)_{m,n}$ denotes the element in row m and column n, and λ is the wavelength. The mapping between m, n, and (v_1, v_2), (u_1, u_2) depends on the dimension of the MIMO system, for example, in the case $M > N$, we get $m = v_1 \cdot V_2 + v_2 + 1$ and $n = u_1 \cdot U_2 + u_2 + 1$. The rest of this section is dedicated to finding an expression for the different path lengths. The procedure employed is based on pure geometrical considerations.

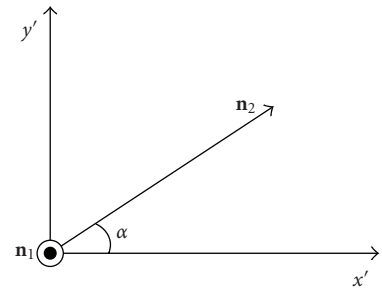

Figure 3: Geometrical illustration of the second principal direction of the URA.

We start by describing the geometry of a single URA; afterwards, two such URAs are utilized to describe the communication link. We define the local origo to be at the lower corner of the URA, and the first principal direction as shown in Figure 2, where we have employed spherical coordinates to describe the direction with the angles $\theta \in [0, \pi/2]$ and $\phi \in [0, 2\pi]$. The unit vector for the first principal direction $\mathbf{n}_1$, with respect to the Cartesian coordinate system in Figure 2, is given by [16, page 252]

$$\mathbf{n}_1 = \sin\theta\cos\phi\, \mathbf{n}_x + \sin\theta\sin\phi\, \mathbf{n}_y + \cos\theta\, \mathbf{n}_z, \tag{6}$$

where $\mathbf{n}_x$, $\mathbf{n}_y$, and $\mathbf{n}_z$ denote the unit vectors in their respective directions.

The second principal direction has to be orthogonal to the first; thus we know that $\mathbf{n}_2$ is in the plane, which is orthogonal to $\mathbf{n}_1$. The two axes in this orthogonal plane are referred to as x' and y'. The plane is illustrated in Figure 3, where $\mathbf{n}_1$ is coming perpendicularly out of the plane, and we have introduced the third angle α to describe the angle between the x'-axis and the second principal direction. To fix this plane described by the x'- and y'-axis to the Cartesian coordinate system in Figure 2, we choose the x'-axis to be orthogonal to the z-axis, that is, placing the x'-axis in the xy-plane. The x' unit vector then becomes

$$\mathbf{n}_{x'} = \frac{1}{|\mathbf{n}_1 \times \mathbf{n}_z|} \mathbf{n}_1 \times \mathbf{n}_z = \sin\phi \mathbf{n}_x - \cos\phi \mathbf{n}_y. \tag{7}$$

Since origo is defined to be at the lower corner of the URA, we require $\alpha \in [\pi, 2\pi]$. Further, we get the y' unit vector

$$\begin{aligned} \mathbf{n}_{y'} &= \frac{1}{|\mathbf{n}_1 \times \mathbf{n}_{x'}|} \mathbf{n}_1 \times \mathbf{n}_{x'} \\ &= \cos\theta\cos\phi \mathbf{n}_x + \cos\theta\sin\phi \mathbf{n}_y - \sin\theta \mathbf{n}_z. \end{aligned} \tag{8}$$

Note that when $\theta = 0$ and $\phi = \pi/2$, then $\mathbf{n}_{x'} = \mathbf{n}_x$ and $\mathbf{n}_{y'} = \mathbf{n}_y$. Based on this description, we observe from Figure 3 that the second principal direction has the unit vector

$$\mathbf{n}_2 = \cos\alpha \mathbf{n}_{x'} + \sin\alpha \mathbf{n}_{y'}. \tag{9}$$

These unit vectors, $\mathbf{n}_1$ and $\mathbf{n}_2$, can now be employed to describe the position of any antenna in the URA. The position difference, relative to the local origo in Figure 2, between

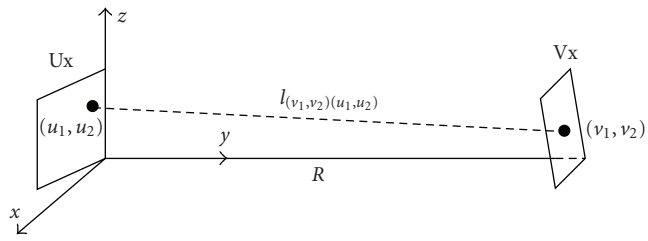

Figure 4: The transmission system investigated.

two neighboring antennas placed in the first principal direction is

$$\begin{aligned}\mathbf{k}^{(1)} &= d^{(1)}\mathbf{n}_1 \\ &= d^{(1)}\left(\sin\theta\cos\phi\mathbf{n}_x + \sin\theta\sin\phi\mathbf{n}_y + \cos\theta\mathbf{n}_z\right),\end{aligned} \tag{10}$$

where $d^{(1)}$ is the distance between two neighboring antennas in the first principal direction. The corresponding position difference in the second principal direction is

$$\begin{aligned}\mathbf{k}^{(2)} = d^{(2)}\mathbf{n}_2 = d^{(2)}\big((&\cos\alpha\sin\phi + \sin\alpha\cos\theta\cos\phi)\mathbf{n}_x \\ &+ (\sin\alpha\cos\theta\sin\phi - \cos\alpha\cos\phi)\mathbf{n}_y \\ &- \sin\alpha\sin\theta\mathbf{n}_z\big),\end{aligned} \tag{11}$$

where $d^{(2)}$ is the distance between the antennas in the second principal direction. $d^{(1)}$ and $d^{(2)}$ can of course take different values, both at the Ux and at the Vx; thus we get two pairs of such distances.

We now employ two URAs as just described to model the communication link. When defining the reference coordinate system for the communication link, we choose the lower corner of the Ux URA to be the global origo, and the y-axis is taken to be in the direction from the lower corner of the Ux URA to the lower corner of the Vx URA. To determine the z- and x-axes, we choose the first principal direction of the Ux URA to be in the yz-plane, that is, $\phi_U = \pi/2$. The system is illustrated in Figure 4, where R is the distance between the lower corner of the two URAs. To find the path lengths that we are searching for, we define a vector from the global origo to Ux antenna (u_1, u_2) as

$$\mathbf{a}_U^{(u_1,u_2)} = u_1 \cdot \mathbf{k}_U^{(1)} + u_2 \cdot \mathbf{k}_U^{(2)}, \tag{12}$$

and a vector from the global origo to Vx antenna (v_1, v_2) as

$$\mathbf{a}_V^{(v_1,v_2)} = R \cdot \mathbf{n}_y + v_1 \cdot \mathbf{k}_V^{(1)} + v_2 \cdot \mathbf{k}_V^{(2)}. \tag{13}$$

All geometrical parameters in $\mathbf{k}^{(1)}$ and $\mathbf{k}^{(2)}$ $(\theta, \phi, \alpha, d^{(1)}, d^{(2)})$ in these two expressions have a subscript U or V to distinguish between the two sides in the communication link. We can now find the distance between Ux antenna (u_1, u_2) and Vx antenna (v_1, v_2) by taking the Euclidean norm of the vector difference:

$$l_{(v_1,v_2)(u_1,u_2)} = \left\|\mathbf{a}_V^{(v_1,v_2)} - \mathbf{a}_U^{(u_1,u_2)}\right\| \tag{14}$$

$$= \left(l_x^2 + \left(R + l_y\right)^2 + l_z^2\right)^{1/2} \tag{15}$$

$$\approx R + l_y + \frac{l_x^2 + l_z^2}{2R}. \tag{16}$$

Here, l_x, l_y, and l_z represent the distances between the two antennas in these directions when disregarding the distance between the URAs R. In the transition from (15) to (16), we perform a Maclaurin series expansion to the first order of the square root expression, that is, $\sqrt{1+a} \approx 1 + a/2$, which is accurate when $a \ll 1$. We also removed the $2 \cdot l_y$ term in the denominator. Both these approximations are good as long as $R \gg l_x, l_y, l_z$.

It is important to note that the geometrical model just described is general, and allows any orientation of the two URAs used in the communication link. Another interesting observation is that the geometrical model incorporates the case of ULAs, for example, by employing $U_2 = 1$, the Ux array becomes a ULA. This will be exploited in the analysis in the next section. A last but very important observation is that we have taken the spherical nature of the electromagnetic wave propagation into account, by applying the actual distance between the Tx and Rx antennas when considering the received phase. Consequently, we have not put any restrictions on the rank of $\mathbf{H}_{\text{LOS}}$, that is, $\text{rank}(\mathbf{H}_{\text{LOS}}) \in \{1, 2, \ldots, U\}$ [11].

4. OPTIMAL URA/ULA DESIGN

In this section, we derive equations for the optimal URA/ULA design with respect to MI when transmitting over a pure LOS MIMO channel. From (2), we know that the important channel parameter with respect to MI is the $\{\mu_p\}$. Further, in [17, page 295], it is shown that the maximal MI is achieved when the $\{\mu_p\}$ are all equal. This situation occurs when all the vectors $\mathbf{h}_{(u_1,u_2)}$ (i.e., columns (rows) of $\mathbf{H}_{\text{LOS}}$ when $M > N$ $(M \leq N)$), containing the channel response between one Ux antenna (u_1, u_2) and all the Vx antennas, that is,

$$\begin{aligned}&\mathbf{h}_{(u_1,u_2)} \\ &= \left[e^{(j2\pi/\lambda)l_{(0,0)(u_1,u_2)}}, e^{(j2\pi/\lambda)l_{(0,1)(u_1,u_2)}}, \ldots, e^{(j2\pi/\lambda)l_{((V_1-1),(V_2-1))(u_1,u_2)}}\right]^T,\end{aligned} \tag{17}$$

are orthogonal to each other, resulting in $\mu_p = V$, for $p \in \{1, \ldots, U\}$. Here, $(\cdot)^T$ is the vector transpose operator. This requirement is actually the motivation behind the choice to distinguish between Ux and Vx instead of Tx and Rx. By basing the analysis on Ux and Vx, we get one general solution, instead of getting one solution valid for $M > N$ and another for $M \leq N$.

When the orthogonality requirement is fulfilled, all the U subchannels are orthogonal to each other. When doing spatial multiplexing on these U orthogonal subchannels, the optimal detection scheme actually becomes the matched filter,

that is, $\mathbf{H}_{\mathrm{LOS}}^{H}$. The matched filter results in no interference between the subchannels due to the orthogonality, and at the same time maximizes the SNR on each of the subchannels (maximum ratio combining).

A consequence of the orthogonality requirement is that the inner product between any combination of two different such vectors should be equal to zero. This can be expressed as $\mathbf{h}^{H}_{(u_{1_b},u_{2_b})}\mathbf{h}_{(u_{1_a},u_{2_a})} = 0$, where the subscripts a and b are employed to distinguish between the two different Ux antennas. The orthogonality requirement can then be written as

$$\sum_{\nu_1=0}^{V_1-1}\sum_{\nu_2=0}^{V_2-1} e^{j2\pi/\lambda\left(l_{(\nu_1,\nu_2)(u_{1_a},u_{2_a})}-l_{(\nu_1,\nu_2)(u_{1_b},u_{2_b})}\right)} = 0. \tag{18}$$

By factorizing the path length difference in the parentheses in this expression with respect to ν_1 and ν_2, it can be written in the equivalent form

$$\sum_{\nu_1=0}^{V_1-1} e^{j2\pi(\hat{\beta}_{11}+\hat{\beta}_{12})\nu_1} \cdot \sum_{\nu_2=0}^{V_2-1} e^{j2\pi(\hat{\beta}_{21}+\hat{\beta}_{22})\nu_2} = 0, \tag{19}$$

where $\hat{\beta}_{ij} = \beta_{ij}(u_{j_b} - u_{j_a})$, and the different β_{ij}s are defined as follows:[4]

$$\beta_{11} = \frac{d_V^{(1)} d_U^{(1)} V_1}{\lambda R}\cos\theta_V \cos\theta_U, \tag{20}$$

$$\beta_{12} = \frac{d_V^{(1)} d_U^{(2)} V_1}{\lambda R}\big[\sin\theta_V \cos\phi_V \cos\alpha_U - \cos\theta_V \sin\alpha_U \sin\theta_U\big], \tag{21}$$

$$\beta_{21} = -\frac{d_V^{(2)} d_U^{(1)} V_2}{\lambda R}\sin\alpha_V \sin\theta_V \cos\theta_U, \tag{22}$$

$$\beta_{22} = \frac{d_V^{(2)} d_U^{(2)} V_2}{\lambda R}\big[\cos\alpha_U \cos\alpha_V \sin\phi_V + \cos\alpha_U \sin\alpha_V \cos\theta_V \cos\phi_V + \sin\alpha_V \sin\alpha_U \sin\theta_V \sin\theta_U\big]. \tag{23}$$

The orthogonality requirement in (19) can be simplified by employing the expression for a geometric sum [16, page 192] and the relation $\sin x = (e^{jx} - e^{-jx})/2j$ [16, page 128] to

$$\underbrace{\frac{\sin\left[\pi(\hat{\beta}_{11}+\hat{\beta}_{12})\right]}{\sin\left[(\pi/V_1)(\hat{\beta}_{11}+\hat{\beta}_{12})\right]}}_{=\zeta_1} \cdot \underbrace{\frac{\sin\left[\pi(\hat{\beta}_{21}+\hat{\beta}_{22})\right]}{\sin\left[(\pi/V_2)(\hat{\beta}_{21}+\hat{\beta}_{22})\right]}}_{=\zeta_2} = 0. \tag{24}$$

Orthogonal subchannels, and thus maximum MI, are achieved if (24) is fulfilled for all combinations of (u_{1_a}, u_{2_a}) and (u_{1_b}, u_{2_b}), except when $(u_{1_a}, u_{2_a}) = (u_{1_b}, u_{2_b})$.

[4] This can be verified by employing the approximate path length from (16) in (18).

The results above clearly show how achieving orthogonal subchannels is dependent on the geometrical parameters, that is, the design of the antenna arrays. By investigating (20)–(23) closer, we observe the following inner product relation:

$$\beta_{ij} = \frac{V_i}{\lambda R}\hat{\mathbf{k}}_U^{(j)T}\hat{\mathbf{k}}_V^{(i)} \quad \forall i, j \in \{1, 2\}, \tag{25}$$

where $\hat{\mathbf{k}}^{(i)} = k_x^{(i)}\mathbf{n}_x + k_z^{(i)}\mathbf{n}_z$, that is, the vectors defined in (10) and (11) where the y-term is set equal to zero. Since solving (24) is dependent on applying correct values of β_{ij}, we see from (25) that it is the extension of the arrays in the x- and z-direction that are crucial with respect to the design of orthogonal subchannels. Moreover, the optimal design is independent of the array extension in the y-direction (direction of transmission). The relation in (25) will be exploited in the analysis to follow to give an alternative projection view on the results.

Both ζ_1 and ζ_2, which are defined in (24), are $\sin(x)/\sin(x/V_i)$ expressions. For these to be zero, the $\sin(x)$ in the nominator must be zero, while the $\sin(x/V_i)$ in the denominator is non-zero, which among other things leads to requirements on the dimensions of the URAs/ULAs, as will be seen in the next subsections. Furthermore, ζ_1 and ζ_2 are periodic functions, thus (24) has more than one solution. We will focus on the solution corresponding to the smallest arrays, both because we see this as the most interesting case from an implementation point of view, and because it would not be feasible to investigate all possible solutions of (24). From (20)–(23), we see that the array size increases with increasing β_{ij}, therefore, in this paper, we will restrict the analysis to the case where the relevant $|\beta_{ij}| \leq 1$, which are found, by investigating (24), to be the smallest values that produce solutions. In the next four subsections, we will systematically go through the possible different combinations of URAs and ULAs in the communications link, and give solutions of (24) if possible.

4.1. ULA at Ux and ULA at Vx

We start with the simplest case, that is, both Ux and Vx employing ULAs. This is equivalent to the scenario we studied in [8]. In this case, we have $U_2 = 1$ giving $\hat{\beta}_{12} = \hat{\beta}_{22} = 0$, and $V_2 = 1$ giving $\zeta_2 = 1$, therefore, we only need to consider $\hat{\beta}_{11}$. Studying (24), we find that the only solution with our array size restriction is $|\beta_{11}| = 1$, that is,

$$d_V^{(1)} d_U^{(1)} = \frac{\lambda R}{V_1 \cos\theta_V \cos\theta_U}, \tag{26}$$

which is identical to the result derived in [8]. The solution is given as a product $d_U\, d_V$, and in accordance with [8], we refer to this product as the *antenna separation product* (ASP). When the relation in (26) is achieved, we have the optimal design in terms of MI, corresponding to orthogonal LOS subchannels.

Projection view

Motivated by the observation in (25), we reformulate (26) as $(d_V^{(1)} \cos\theta_V) \cdot (d_U^{(1)} \cos\theta_U) = \lambda R/V_1$. Consequently, we observe that the the product of the antenna separations projected along the local z-axis at both sides of the link should be equal to $\lambda R/V_1$. The z-direction is the only direction of relevance due to the fact that it is only the array extension in the xz-plane that is of interest (cf. (25)), and the fact that the first (and only) principal direction at the Ux is in the yz-plane (i.e., $\phi_U = \pi/2$).

4.2. URA at Ux and ULA at Vx

Since Vx is a ULA, we have $V_2 = 1$ giving $\zeta_2 = 1$, thus to get the optimal design, we need $\zeta_1 = 0$. It turns out that with the aforementioned array size restriction ($|\beta_{ij}| \leq 1$), it is not possible to find a solution to this problem, for example, by employing $|\beta_{11}| = |\beta_{12}| = 1$, we observe that $\zeta_1 = 0$ for most combinations of Ux antennas, except when $u_{1_a} + u_{2_a} = u_{1_b} + u_{2_b}$, which gives $\zeta_1 = V_1$. By examining this case a bit closer, we find that the antenna elements in the URA that are correlated, that is, giving $\zeta_1 = V_1$, are the diagonal elements of the URA. Consequently, the optimal design is not possible in this case.

Projection view

By employing the projection view, we can reveal the reason why the diagonal elements become correlated, and thus why a solution is not possible. Actually, it turns out that the diagonal of the URA projected on to the xz-plane is perpendicular to the ULA projected on to the xz-plane when $|\beta_{11}| = |\beta_{12}| = 1$. This can be verified by applying (25) to show the following relation:

$$\underbrace{\left(\widehat{\mathbf{k}}_U^{(1)} - \widehat{\mathbf{k}}_U^{(2)}\right)^T}_{\text{diagonal of URA}} \cdot \widehat{\mathbf{k}}_V^{(1)} = 0. \tag{27}$$

Moreover, the diagonal of the URA can be viewed as a ULA, and when two ULAs are perpendicular aligned in space, the ASP goes towards infinity (this can be verified by employing $\theta_V \to \pi/2$ in (26)). This indicates that it is not possible to do the optimal design when this perpendicularity is present.

4.3. ULA at Ux and URA at Vx

As mentioned earlier, a ULA at Ux gives $U_2 = 1$, resulting in $(u_{2_b} - u_{2_a}) = 0$, and thus $\widehat{\beta}_{12} = \widehat{\beta}_{22} = 0$. Investigating the remaining expression in (24), we see that the optimal design is achieved when $|\beta_{11}| = 1$ if $V_1 \geq U$, giving $\zeta_1 = 0$, or $|\beta_{21}| = 1$ if $V_2 \geq U$, giving $\zeta_2 = 0$, that is,

$$d_V^{(1)} d_U^{(1)} = \frac{\lambda R}{V_1 \cos\theta_V \cos\theta_U} \quad \text{if } V_1 \geq U, \text{ or} \tag{28}$$

$$d_V^{(2)} d_U^{(1)} = \frac{\lambda R}{V_2 \sin\theta_V \,|\, \sin\alpha_V \,|\, \cos\theta_U} \quad \text{if } V_2 \geq U. \tag{29}$$

Furthermore, the optimal design is also achieved if both the above ASP equations are fulfilled simultaneously, and either $q/V_1 \notin \mathbb{Z}$ or $q/V_2 \notin \mathbb{Z}$, for all $q < U$. This guarantees either $\zeta_1 = 0$ or $\zeta_2 = 0$ for all combinations of u_{1_a} and u_{1_b}.

Projection view

A similar reformulation as performed in Section 4.1 can be done for this scenario. We see that both ASP equations, (28) and (29), contain the term $\cos\theta_U$, which projects the antenna distance at the Ux side on the z-axis. The other trigonometric functions project the Vx antenna separation on to the z-axis, either based on the first principal direction (28) or based on the second principal direction (29).

4.4. URA at Ux and URA at Vx

In this last case, when both Ux and Vx are URAs, we have $U_1, U_2, V_1, V_2 > 1$. By investigating (20)–(24), we observe that in order to be able to solve (24), at least one β_{ij} must be zero. This indicates that the optimal design in this case is only possible for some array orientations, that is, values of θ, ϕ, and α, giving one $\beta_{ij} = 0$. To solve (24) when one $\beta_{ij} = 0$, we observe the following requirement on the β_{ij} s: $|\beta_{11}| = |\beta_{22}| = 1$ and $V_1 \geq U_1$, $V_2 \geq U_2$ or $|\beta_{12}| = |\beta_{21}| = 1$ and $V_1 \geq U_2$, $V_2 \geq U_1$.

This is best illustrated through an example. For instance, we can look at the case where $\alpha_V = 0$, which results in $\beta_{21} = 0$. From (24), we observe that when $\beta_{21} = 0$ and $|\beta_{22}| = 1$, we always have $\zeta_2 = 0$ if $V_2 \geq U_2$, except when $(u_{2_b} - u_{2_a}) = 0$. Thus to get orthogonality in this case as well, we need $|\beta_{11}| = 1$ and $V_1 \geq U_1$. Therefore, the optimal design for this example becomes

$$d_V^{(1)} d_U^{(1)} = \frac{\lambda R}{V_1 \cos\theta_V \cos\theta_U}, \quad V_1 \geq U_1, \tag{30}$$

$$d_V^{(2)} d_U^{(2)} = \frac{\lambda R}{V_2 \,|\, \cos\alpha_U \sin\phi_V \,|}, \quad V_2 \geq U_2. \tag{31}$$

The special case of two broadside URAs is revealed by further setting $\alpha_U = 0$, $\theta_U = 0$, $\theta_V = 0$, and $\phi_V = \pi/2$ in (30) and (31). The optimal ASPs are then given by

$$d_V^{(1)} d_U^{(1)} = \frac{\lambda R}{V_1}, \quad V_1 \geq U_1; \qquad d_V^{(2)} d_U^{(2)} = \frac{\lambda R}{V_2}, \quad V_2 \geq U_2. \tag{32}$$

This corresponds exactly to the result given in [10], which shows the generality of the equations derived in this work and how they contain previous work as special cases.

Projection view

We now look at the example where $\alpha_V = 0$ with a projection view. We observe that in (30), both antenna separations in the first principal directions are projected along the z-axis at Ux and Vx, and the product of these two distances should be equal to $\lambda R/V_1$. In (31), the antenna separations along the second principal direction are projected on the x-axis at Ux

and Vx, and the product should be equal to $\lambda R/V_2$. These results clearly show that it is the extension of the arrays in the plane perpendicular to the transmission direction that is crucial. Moreover, the correct extension in the xz-plane is dependent on the wavelength, transmission distance, and dimension of the Vx.

4.5. Practical considerations

We observe that the optimal design equations from previous subsections are all on the same form, that is, $d_V\, d_U = \lambda R/V_i X$, where X is given by the orientation of the arrays. A first comment is that utilizing the design equations to achieve high performance MIMO links is best suited for fixed systems (such as wireless LANs with LOS conditions,[5] broadband wireless access, radio relay systems, etc.) since the optimal design is dependent on both the orientation and the Tx-Rx distance. Another important aspect is the size of the arrays. To keep the array size reasonable,[6] the product λR should not be too large, that is, the scheme is best suited for high frequency and/or short range communications. Note that these properties agree well with systems that have a fairly high probability of having a strong LOS channel component present. The orientation also affects the array size, for example, if $X \to 0$, the optimal antenna separation goes towards infinity. As discussed in the previous sections, it is the array extension in the xz-plane that is important with respect to performance, consequently, placing the arrays in this plane minimizes the size required.

Furthermore, we observe that in most cases, even if one array is fully specified, the optimal design is still possible. For instance, from (30) and (31), we see that if $d^{(1)}$ and $d^{(2)}$ are given for one URA, we can still do the optimal design by choosing appropriate values for $d^{(1)}$ and $d^{(2)}$ for the other URA. This is an important property for centralized systems utilizing *base stations* (BSs), which allows for the optimal design for the different communication links by adapting the subscriber units' arrays to the BS array.

5. EIGENVALUES OF W

As in the previous two sections, we focus on the pure LOS channel matrix in this analysis. From Section 4, we know that in the case of optimal array design, we get $\mu_p = V$ for all p, that is, all the eigenvalues of $\mathbf{W}$ are equal to V. An interesting question now is: What happens to the μ_p s if the design deviates from the optimal as given in Section 4? In our analysis of nonoptimal design, we make use of $\{\beta_{ij}\}$. From above, we know that the optimal design, requiring the smallest antenna arrays, was found by setting the relevant $|\beta_{ij}|$ equal to zero or unity, depending on the transmission scenario. Since $\{\beta_{ij}\}$ are functions of the geometrical parameters, studying the deviation from the optimal design is equivalent to studying the behavior of $\{\mu_p\}_{p=1}^{U}$, when the relevant β_{ij}s deviate from the optimal ones. First, we give a simplified expression for the eigenvalues of $\mathbf{W}$ as functions of β_{ij}. Then, we look at an interesting special case where we give explicit analytical expressions for $\{\mu_p\}_{p=1}^{U}$ and describe a method for characterizing nonoptimal designs.

We employ the path length found in (16) in the $\mathbf{H}_{\text{LOS}}$ model. As in [8], we utilize the fact that the eigenvalues of the previously defined Hermitian matrix $\mathbf{W}$ are the same as for a real symmetric matrix $\widehat{\mathbf{W}}$ defined by $\mathbf{W} = \mathbf{B}^H\widehat{\mathbf{W}}\mathbf{B}$, where $\mathbf{B}$ is a unitary matrix.[7] For the URA case studied in this paper, it is straightforward to show that the elements of $\widehat{\mathbf{W}}$ are (cf. (24))

$$(\widehat{\mathbf{W}})_{k,l} = \frac{\sin\left[\pi(\hat{\beta}_{11}+\hat{\beta}_{12})\right]}{\sin\left[(\pi/V_1)(\hat{\beta}_{11}+\hat{\beta}_{12})\right]} \cdot \frac{\sin\left[\pi(\hat{\beta}_{21}+\hat{\beta}_{22})\right]}{\sin\left[(\pi/V_2)(\hat{\beta}_{21}+\hat{\beta}_{22})\right]}, \tag{33}$$

where $k = u_{1_a}U_2 + u_{2_a} + 1$ and $l = u_{1_b}U_2 + u_{2_b} + 1$. We can now find the eigenvalues $\{\mu_p\}_{p=1}^{U}$ of $\mathbf{W}$ by solving $\det(\widehat{\mathbf{W}} - \mathbf{I}_U\mu) = 0$, where $\det(\cdot)$ is the matrix determinant operator. Analytical expressions for the eigenvalues can be calculated for all combinations of ULA and URA communication links by using a similar procedure to that in Section 4. The eigenvalue expressions become, however, more and more involved for increasing values of U.

5.1. Example: $\beta_{11} = \beta_{22} = 0$ or $\beta_{12} = \beta_{21} = 0$

As an example, we look at the special case that occurs when $\beta_{11} = \beta_{22} = 0$ or $\beta_{12} = \beta_{21} = 0$. This is true for some geometrical parameter combinations, when employing URAs both at Ux and Vx, for example, the case of two broadside URAs. In this situation, we see that the matrix $\widehat{\mathbf{W}}$ from (33) can be written as a Kronecker product of two square matrices [10], that is,

$$\widehat{\mathbf{W}} = \widehat{\mathbf{W}}_1 \otimes \widehat{\mathbf{W}}_2, \tag{34}$$

where

$$(\widehat{\mathbf{W}}_i)_{k,l} = \frac{\sin\left(\pi\beta_{ij}(k-l)\right)}{\sin\left(\pi(\beta_{ij}/V_i)(k-l)\right)}. \tag{35}$$

Here, $k, l \in \{1, 2, \ldots, U_j\}$ and the subscript $j \in \{1, 2\}$ is dependent on β_{ij}. If $\widehat{\mathbf{W}}_1$ has the eigenvalues $\{\mu_{p_1}^{(1)}\}_{p_1=1}^{U_j}$, and $\widehat{\mathbf{W}}_2$ has the eigenvalues $\{\mu_{p_2}^{(2)}\}_{p_2=1}^{U_j}$, we know from matrix theory that the matrix $\widehat{\mathbf{W}}$ has the eigenvalues

$$\mu_p = \mu_{p_1}^{(1)} \cdot \mu_{p_2}^{(2)}, \quad \forall\, p_1, p_2. \tag{36}$$

[5] This is of course not the case for all wireless LANs.

[6] What is considered as reasonable, of course, depends on the application, and may, for example, vary for WLAN, broadband wireless access, and radio relay systems.

[7] This implies that $\det(\mathbf{W} - \lambda\mathbf{I}) = 0 \Rightarrow \det(\mathbf{B}^H\widehat{\mathbf{W}}\mathbf{B} - \lambda\mathbf{B}^H\mathbf{I}\mathbf{B}) = 0 \Rightarrow \det(\widehat{\mathbf{W}} - \lambda\mathbf{I}) = 0$.

Expressions for $\mu_{p_i}^{(i)}$ were given in [8] for $U_j = 2$ and $U_j = 3$. For example, for $U_j = 2$ we get the eigenvalues

$$\mu_1^{(i)} = V_i + \frac{\sin(\beta_{ij}\pi)}{\sin(\beta_{ij}(\pi/V_i))}, \qquad \mu_2^{(i)} = V_i - \frac{\sin(\beta_{ij}\pi)}{\sin(\beta_{ij}(\pi/V_i))}. \tag{37}$$

In this case, we only have two nonzero β_{ij}s, which we from now on, denote β_1 and β_2, that fully characterize the URA design. The optimal design is obtained when both $|\beta_i|$ are equal to unity, while the actual antenna separation is too small (large) when $|\beta_i| > 1$ ($|\beta_i| < 1$). This will be applied in the results section to analyze the design.

There can be several reasons for $|\beta_i|$ to deviate from unity (0 dB). For example, the optimal ASP may be too large for practical systems so that a compromise is needed, or the geometrical parameters may be difficult to determine with sufficient accuracy. A third reason for nonoptimal array design may be the wavelength dependence. A communication system always occupies a nonzero bandwidth, while the antenna distance can only be optimal for one single frequency. As an example, consider the 10.5 GHz-licensed band (10.000–10.680 GHz [18]). If we design a system for the center frequency, the deviation for the lower frequency yields $\lambda_{\text{low}}/\lambda_{\text{design}} = f_{\text{design}}/f_{\text{low}} = 10.340/10.000 = 1.034 = 0.145$ dB. Consequently, this bandwidth dependency only contribute to a 0.145 dB deviation in the $|\beta_i|$ in this case, and in Section 6, we will see that this has almost no impact on the performance of the MIMO system.

6. RESULTS

In this section, we will consider the example of a 4×4 MIMO system with URAs both at Ux and Vx, that is, $U_1 = U_2 = V_1 = V_2 = 2$. Further, we set $\theta_V = \theta_U = 0$, which gives $\beta_{12} = \beta_{21} = 0$; thus we can make use of the results from the last subsection, where the nonoptimal design is characterized by β_1 and β_2.

Analytical expressions for $\{\mu_p\}_{p=1}^4$ in the pure LOS case are found by employing (37) in (36). The square roots of the eigenvalues (i.e., singular values of $\mathbf{H}_{\text{LOS}}$) are plotted as a function of $|\beta_1| = |\beta_2|$ in Figure 5. The lines represent the analytical expressions, while the circles are determined by using a numerical procedure to find the singular values when the *exact* path length from (15) is employed in $\mathbf{H}_{\text{LOS}}$. The parameters used in the exact path length case are as follows: $\phi_V = \pi/2$, $\alpha_U = \pi$, $\alpha_V = \pi$, $R = 500$ m, $d_U^{(1)} = 1$ m, $d_U^{(2)} = 1$ m, $\lambda = 0.03$ m, while $d_V^{(1)}$ and $d_V^{(2)}$ are chosen to get the correct values of $|\beta_1|$ and $|\beta_2|$.

The figure shows that there is a perfect agreement between the analytical singular values based on approximate path lengths from (16), and the singular values found based on exact path lengths from (15). We see how the singular values spread out as the design deviates further and further from the optimal (decreasing $|\beta_i|$), and for small $|\beta_i|$, we get $\text{rank}(\mathbf{H}_{\text{LOS}}) = 1$, which we refer to as a total design mismatch. In the figure, the solid line in the middle represents two singular values, as they become identical in the present case ($|\beta_1| = |\beta_2|$). This is easily verified by observing the symmetry in the analytical expressions for the eigenvalues. For $|\beta_i| > 1$, we experience some kind of periodic behavior; this is due to the fact that (24) has more than one solution. However, in this paper, we introduced a size requirement on the arrays, thus we concentrate on the solutions where $|\beta| \leq 1$.

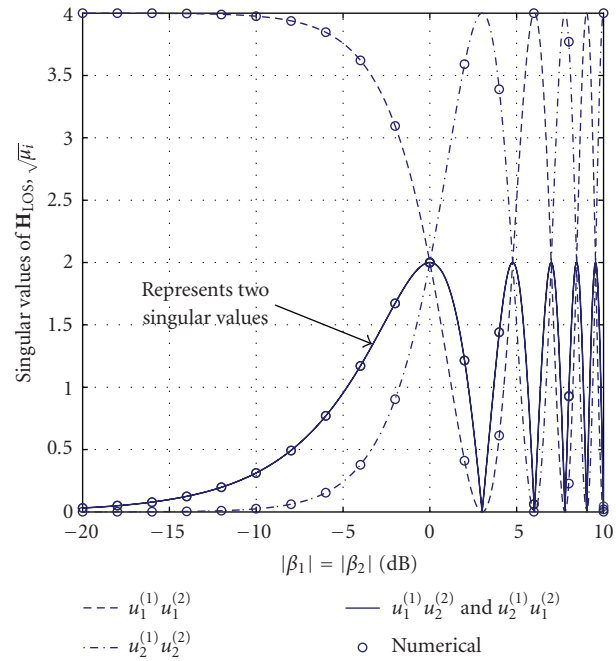

FIGURE 5: The singular values of $\mathbf{H}_{\text{LOS}}$ for the 4×4 MIMO system as a function of $|\beta_1| = |\beta_2|$, both exactly found by a numerical procedure and the analytical from Section 5.

When $K \neq \infty$ in (4), the MI from (2) becomes a random variable. We characterize the random MI by the MI *cumulative distribution function* (CDF), which is defined as the probability that the MI falls below a given threshold, that is, $F(\mathcal{I}_{\text{th}}) = \Pr[\mathcal{I} < \mathcal{I}_{\text{th}}]$ [5]. All CDF curves plotted in the next figures are based on 50 000 channel realizations.

We start by illustrating the combined influence of $|\beta_i|$ and the Ricean K-factor. In Figure 6, we show $F(\mathcal{I}_{\text{th}})$ for the optimal design case ($|\beta_1| = |\beta_2| = 0$ dB), and for the total design mismatch ($|\beta_1| = |\beta_2| = -30$ dB).

The figure shows that the design of the URAs becomes more and more important as the K-factor increases. This is because it increases the influence of $\mathbf{H}_{\text{LOS}}$ on $\mathbf{H}$ (cf. (4)). We also observe that the MI increases for the optimal design case when the K-factor increases, while the MI decreases for increasing K-factors in the total design mismatch case. This illustrates the fact that the pure LOS case outperforms the uncorrelated Rayleigh case when we do optimal array design (i.e., orthogonal LOS subchannels).

In Figure 7, we illustrate how $F(\mathcal{I}_{\text{th}})$ changes when we have different combinations of the two $|\beta_i|$. We see how the MI decreases when $|\beta_i|$ decreases. In this case, the Ricean K-factor is 5 dB, and from Figure 6, we know that the MI would be even more sensitive to $|\beta_i|$ for larger K-factors. From the figure, we observe that even with some deviation from the

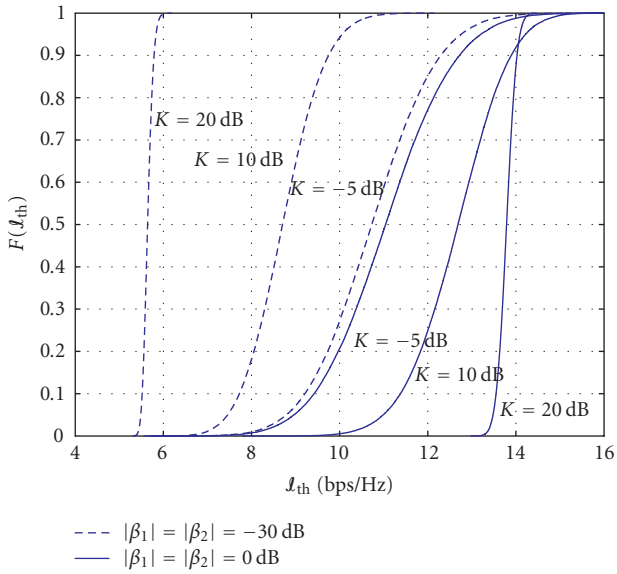

FIGURE 6: The MI CDF for the 4×4 MIMO system when $\overline{\gamma} = 10$ dB.

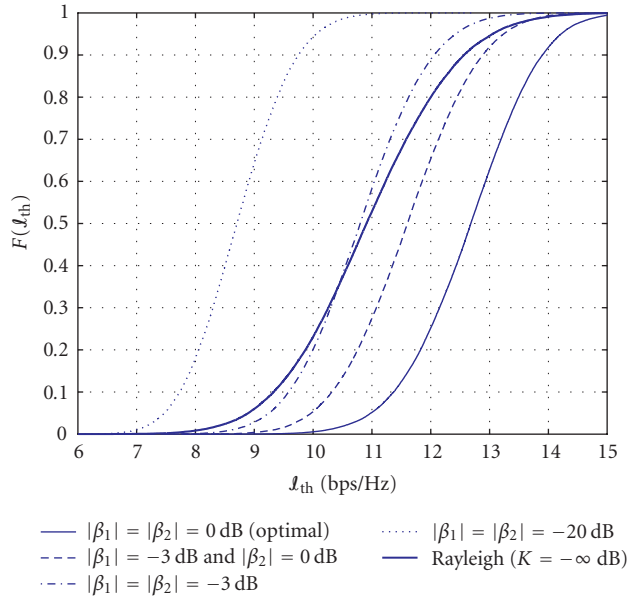

FIGURE 7: The MI CDF for the 4×4 MIMO system when $\overline{\gamma} = 10$ dB and $K = 5$ dB (except for the Rayleigh channel where $K = -\infty$ dB).

optimal design, we get higher MI compared to the case of uncorrelated Rayleigh subchannels.

7. CONCLUSIONS

Based on the new general geometrical model introduced for the *uniform rectangular array* (URA), which also incorporates the *uniform linear array* (ULA), we have investigated the optimal design for *line-of-sight* (LOS) channels with respect to mutual information for all possible combinations of URA and ULA at transmitter and receiver. The optimal design based on correct separation between the antennas (d_U and d_V) is possible in several interesting cases. Important parameters with respect to the optimal design are the wavelength, the transmission distance, and the array dimensions in the plane perpendicular to the transmission direction.

Furthermore, we have characterized and investigated the consequence of nonoptimal design, and in the general case, we gave simplified expressions for the pure LOS eigenvalues as a function of the design parameters. In addition, we derived explicit analytical expressions for the eigenvalues for some interesting cases.

ACKNOWLEDGMENTS

This work was funded by Nera with support from the Research Council of Norway (NFR), and partly by the BEATS project financed by the NFR, and the NEWCOM Network of Excellence. Some of this material was presented at the IEEE Signal Processing Advances in Wireless Communications (SPAWC), Cannes, France, July 2006.

REFERENCES

[1] G. J. Foschini and M. J. Gans, "On limits of wireless communications in a fading environment when using multiple antennas," *Wireless Personal Communications*, vol. 6, no. 3, pp. 311–335, 1998.

[2] E. Telatar, "Capacity of multiantenna Gaussian channels," Tech. Memo, AT&T Bell Laboratories, Murray Hill, NJ, USA, June 1995.

[3] T. Kaiser, "When will smart antennas be ready for the market? Part I," *IEEE Signal Processing Magazine*, vol. 22, no. 2, pp. 87–92, 2005.

[4] T. Kaiser, "When will smart antennas be ready for the market? Part II—results," *IEEE Signal Processing Magazine*, vol. 22, no. 6, pp. 174–176, 2005.

[5] D. Gesbert, M. Shafi, D.-S. Shiu, P. J. Smith, and A. Naguib, "From theory to practice: an overview of MIMO space-time coded wireless systems," *IEEE Journal on Selected Areas in Communications*, vol. 21, no. 3, pp. 281–302, 2003.

[6] D. Gesbert, "Multipath: curse or blessing? A system performance analysis of MIMO wireless systems," in *Proceedings of the International Zurich Seminar on Communications (IZS '04)*, pp. 14–17, Zurich, Switzerland, February 2004.

[7] P. F. Driessen and G. J. Foschini, "On the capacity formula for multiple input-multiple output wireless channels: a geometric interpretation," *IEEE Transactions on Communications*, vol. 47, no. 2, pp. 173–176, 1999.

[8] F. Bøhagen, P. Orten, and G. E. Øien, "Design of optimal high-rank line-of-sight MIMO channels," *IEEE Transactions on Wireless Communications*, vol. 6, no. 4, pp. 1420–1425, 2007.

[9] F. Bøhagen, P. Orten, and G. E. Øien, "Construction and capacity analysis of high-rank line-of-sight MIMO channels," in *Proceedings of the IEEE Wireless Communications and Networking Conference (WCNC '05)*, vol. 1, pp. 432–437, New Orleans, La, USA, March 2005.

[10] P. Larsson, "Lattice array receiver and sender for spatially orthonormal MIMO communication," in *Proceedings of the IEEE 61st Vehicular Technology Conference (VTC '05)*, vol. 1, pp. 192–196, Stockholm, Sweden, May 2005.

[11] F. Bøhagen, P. Orten, and G. E. Øien, "On spherical vs. plane wave modeling of line-of-sight MIMO channels," to appear in *IEEE Transactions on Communications*.
[12] H. Xu, M. J. Gans, N. Amitay, and R. A. Valenzuela, "Experimental verification of MTMR system capacity in controlled propagation environment," *Electronics Letters*, vol. 37, no. 15, pp. 936–937, 2001.
[13] J.-S. Jiang and M. A. Ingram, "Spherical-wave model for short-range MIMO," *IEEE Transactions on Communications*, vol. 53, no. 9, pp. 1534–1541, 2005.
[14] D. Hosli and A. Lapidoth, "How good is an isotropic Gaussian input on a MIMO Ricean channel?" in *Proceedings IEEE International Symposium on Information Theory (ISIT '04)*, p. 291, Chicago, Ill, USA, June-July 2004.
[15] G. L. Stüber, *Principles of Mobile Communication*, Kluwer Academic Publishers, Norwell, Mass, USA, 2nd edition, 2001.
[16] L. Råde and B. Westergren, *Mathematics Handbook for Science and Engineering*, Springer, Berlin, Germany, 5th edition, 2004.
[17] D. Tse and P. Viswanath, *Fundamentals of Wireless Communication*, Cambridge University Press, Cambridge, UK, 1st edition, 2005.
[18] IEEE 802.16-2004, "IEEE standard for local and metropolitan area networks part 16: air interface for fixed broadband wireless access systems," October 2004.